ARTIFICIAL INTELLIGENCE FOR OPTICAL COHERENCE TOMOGRAPHY ANGIOGRAPHY–BASED DISEASE ACTIVITY PREDICTION IN AGE-RELATED MACULAR DEGENERATION

ANNA HEINKE, MD, PHD,*† HAOCHEN ZHANG, MS,‡ DANIEL DEUSSEN, MD,*†§
CARLO MIGUEL B. GALANG, MD,*† ALEXANDRA WARTER, MD,*†
FRITZ GERALD P. KALAW, MD,*† DIRK-UWE G. BARTSCH, PHD,*† LINGYUN CHENG, MD,*†
CHEOLHONG AN, PHD,‡ TRUONG NGUYEN, PHD,‡
WILLIAM R. FREEMAN, MD*†‡

Purpose: The authors hypothesize that optical coherence tomography angiography (OCTA)–visualized vascular morphology may be a predictor of choroidal neovascularization status in age-related macular degeneration (AMD). The authors thus evaluated the use of artificial intelligence (AI) to predict different stages of AMD disease based on OCTA en face 2D projections scans.

Methods: Retrospective cross-sectional study based on collected 2D OCTA data from 310 high-resolution scans. Based on OCT B-scan fluid and clinical status, OCTA was classified as normal, dry AMD, wet AMD active, and wet AMD in remission with no signs of activity. Two human experts graded the same test set, and a consensus grading between two experts was used for the prediction of four categories.

Results: The AI can achieve 80.36% accuracy on a four-category grading task with 2D OCTA projections. The sensitivity of prediction by AI was 0.7857 (active), 0.7142 (remission), 0.9286 (dry AMD), and 0.9286 (normal) and the specificity was 0.9524, 0.9524, 0.9286, and 0.9524, respectively. The sensitivity of prediction by human experts was 0.4286 active choroidal neovascularization, 0.2143 remission, 0.8571 dry AMD, and 0.8571 normal with specificity of 0.7619, 0.9286, 0.7857, and 0.9762, respectively. The overall AI classification prediction was significantly better than the human (odds ratio = 1.95, $P = 0.0021$).

Conclusion: These data show that choroidal neovascularization morphology can be used to predict disease activity by AI; longitudinal studies are needed to better understand the evolution of choroidal neovascularization and features that predict reactivation. Future studies will be able to evaluate the additional predicative value of OCTA on top of other imaging characteristics (i.e., fluid location on OCT B scans) to help predict response to treatment.

RETINA 44:465–474, 2024

Optical coherence tomography angiography (OCTA) is a relatively new, noninvasive imaging modality that permits visualization of retinal and inner choroidal circulation without the need for the dye injection, based on the principle of mapping erythrocyte movement over time by comparing sequential OCT sagittal scans at a given cross-section.[1] Thanks to its ability to visualize choroidal and retinal microvasculature at micron-scale resolution, and OCTA is increasingly used to detect the choroidal neovascularization (CNV) lesions in neovascular age-related macular degeneration (AMD),[2] which is the most common cause for severe visual loss in industrialized countries.[3] Optical coherence tomography angiography also allows quantification of vascular metrics that correlate with clinical disease severity and progression,

that is it can be used in quantitative assessment of the morphologic changes in CNV vessels in nAMD in response to antivascular endothelial growth factor (anti-VEGF) treatment.[4] Although this modality has provided quantification of healthy vessels and pathology in AMD disease, it is common for OCTA data to contain artifacts that may influence measurement outcomes or defy image interpretation. Artifacts may include projection, motion, signal reduction, and segmentation errors, which have all been recognized.[5] Artifacts compensation can improve the accuracy of the OCTA measurements, and there are strategies developed for their removal.[5,6]

Multiple studies have shown the utility of OCTA for the detection of choroidal neovascular membranes in neovascular AMD. Documented sensitivities for OCTA compared with gold standard fluorescein angiography and structural OCT have ranged from 50% to 87% with corresponding specificities of 91% to 98% for the detection of CNV using commercially available spectral domain devices.[7] Choroidal neovascularizations that were clinically present but not detected by OCTA were found in association with significant subretinal hemorrhage[8] and large pigment epithelial detachment.[9] Thus, the clinical utility of OCTA images alone to assist decision-making in the treatment of CNV is uncertain. Previous studies have shown that en face OCTA images have only a moderate ability to identify CNV and OCTA alone is limited at determining CNV activity as inactive vessels may persist in the absence of frank vascular leakage. Cavichini et al[10] has shown that CNV vessels are often present without leakage and sometimes are not seen despite clinical activity. Although OCTA is currently not considered a golden standard in decision-making in CNV treatment, its noninvasive nature and the ability to detect subclinical pathologic changes[11] make OCTA ideally suited for diagnostic imaging and monitoring.

To validate OCTA metrics with large-scale studies, automation of OCTA analysis based on artificial intelligence (AI) would be beneficial. Fortunately, advances in OCTA are occurring together with similar improvements in image analysis driven by AI and in particularly deep learning–based algorithms.[12] Deep learning (DL) has been applied to ocular imaging, principally fundus photographs and optical coherence tomography (OCT). One of the major ophthalmic diseases which DL techniques have been used for includes AMD.[13] The contemporary applications of AI in OCTA include accurate detection of pathologies such as choroidal neovascularization, precise quantification of retinal perfusion, and reliable disease diagnosis.[12] Most existing OCTA-based AI works focus on segmentation tasks and the removal of different OCTA artifacts.[14] Most of the existing deep learning AMD analysis studies are based on OCT modality. Alqudah et al trained a customized convolutional neural network to classify the SD-OCTs of the retina into five AMD stages.[15] Other studies have used multimodal imaging, such as fundus photograph, OCT B scans, and OCTA projections for AMD detection and grading.[16–18] Our goal was to apply deep learning algorithms to OCTA en face projections to help analyze vascular patterns in CNV. This has been performed manually and vascular density, and branching index have been claimed to be predictive of activity of neovascular AMD.[19,20] AI has not been applied to this. Our purpose was to determine whether deep learning AI can predict different stages of AMD disease and differentiate active from inactive CNV vessels based on OCTA vascular characteristics. Another goal was to determine whether deep learning prediction classifiers correlate with or are superior to human evaluations of vascular characteristics made by experienced ophthalmologists.

Methods

Optical Coherence Tomography Angiography Data Selection and Labeling

This cross-sectional, retrospective, single-institution study was approved by the Institutional Review Board of the University of California San Diego in California, USA, and complied with the Health Insurance Portability and Accountability Act of 1996. All the data that were collected were anonymized for patient's safety. Data collection and analysis were conducted according to the Principles of the Declaration of Helsinki.

Three hundred ten OCTA high-quality en face scans were obtained retrospectively from patients diagnosed

From the *Department of Ophthalmology at the Shiley Eye Institute, University of California at San Diego La Jolla, California; †Joan and Irwin Jacobs Retina Center, La Jolla, California; ‡Department of Electrical and Computer Engineering, University of California San Diego, La Jolla, California; and §University Eye Hospital, Ludwig-Maximillians-University, Munich, Germany.

R01EY033847 (T. Nguyen and W. R. Freeman), UCSD Vision Research Center Core Grant from the National Eye Institute P30EY022589, NIH Grant R01EY016323 (D.-U. G. Bartsch), an unrestricted grant from Research to Prevent Blindness, NY (W. R. Freeman), and unrestricted funds from the UCSD Jacobs Retina Center, OT2OD032644.

None of the authors has any financial/conflicting interests to disclose.

Reprint requests: William R. Freeman, MD, Jacobs Retina Center, 9415 Campus Point Drive, La Jolla, CA 92037; e-mail: wrfreeman@health.ucsd.edu

at Jacobs Retina Center, Shiley Eye Institute, University of California San Diego, San Diego, La Jolla, California between 2021 and 2022. The imaging reports and electronic charts were reviewed for clinical information, such as diagnosis and anti-VEGF treatment information for analysis. Inclusion criteria were age older than 50 years, presence of AMD diagnosis, and the presence of high-quality OCTA scans in the database (defined as lack of motion artifacts and background noise and quality index Q had to be $>$ or = 25).[21,22] Of 400 initially chosen OCTA scans, we excluded 14 scans due to the diagnosis of CNV of the etiology different than AMD (9 myopic CNV, two CNV secondary to central serous chorioretinopathy, and three peripapillary CNV) and 76 scans were excluded due to motion artifacts, incomplete scan, background noise, and poor quality of the scan (defined with quality index Q $<$ 25). Each eye was analyzed independently. The OCTA scans were performed per eye, and exclusion criteria were performed per eye level. In 234 patients, only one eye was included and in 38 patients, both eyes were included in the analysis, giving 310 eyes in total. Thus, only 38 eyes of the 310 were fellow eyes, which have no statistically significant effect on the outcome. Patients were divided into four groups based on clinical classification category. Group 1 was "wet active AMD" including patients with CNV and fluid in B-scan OCT (newly diagnosed treatment naïve as well as patients with fluid on OCT and ongoing anti-VEGF treatment). Group 2 was "wet AMD in remission" including patients with treated CNV without fluid on OCT. Group 3 was dry AMD without CNV and fluid in OCT, and Group 4 was healthy eyes with no AMD or other retinal pathology. Exclusion criteria were eyes with CNV secondary to a disease other than wet AMD and poor-quality OCTA images with artifacts and Q index $<$25. Two retina specialists determined the clinical activity based on information of subretinal and/or intraretinal fluid from OCT B scan from the same day as the OCTA scan was performed. The labeling was based on OCT B-scan information and clinical data gathered from electronic chart review (diagnosis, anti-VEGF treatment) without viewing the OCTA images. This labeling was the "gold standard." Each imaging result was reviewed with the senior retina specialist (W.R.F.), who decided on the diagnosis if there was any disagreement on labeling."

A complete ophthalmologic examination including best-corrected visual acuity using the Early Treatment Diabetic Retinopathy Study chart, slit-lamp biomicroscopy, and indirect ophthalmoscopy following dilatation and retinal imaging including SD-OCT and OCTA centered at the macula using the SPECTRALIS HRA + OCT (Heidelberg Engineering, Heidelberg, Germany) were performed in all eyes. OCTA scan pattern was as follows: number of B-scans = 512, pattern size = 3 × 3 mm/10° × 10°, distance between B-Scans = 6 mm, ART images average = 5. Automated segmentation provided by embedded Heidelberg software was used for segmentation correction. The OCTA scans were exported as 2D en face vascular projections only (superficial, deep, avascular, and choriocapillaris). Before generating the OCTA image of vessels, the automated segmentation of Heidelberg software was reviewed by two retina specialists (same ones who were labeling the data). Each scan was checked for segmentation error directly from Heidelberg SPECTRALIS machine using Heyex two software by scrolling over 512-line B scans. The Bruch membrane line was evaluated. The inner retinal segmentation was not reviewed. If there was a gross or minimal segmentation error of the Bruch membrane, the segmentation was corrected and labeled Y for gross and M for minor segmentation error in Excel spreadsheet. Accurate segmentation with correct delineation of the retinal layers was noted as N—for no error.

Artificial Intelligence Methods

For the AI training, we followed the standard training/validation/testing data split protocol: Starting from a total of 310 samples, we first selected 56 samples for testing. Then, within the remaining 254 samples, we selected the validation set to form the 5-fold validation experiment. Thus, the 56 testing samples are pure unseen data for AI.

We use the same 56-sample test set for both AI and human performance evaluation.

The training, validation, and test sets were assigned randomly, so it is possible that scans from the same patient in different time were assigned to different subsets. However, it is worth noting that the influence of scans from the same patient is negligible because of two facts: First, even if the scans are from the same patient, they can be in different categories, and second, those scans are the minority in our data set.

We obtained 254 OCTA images, and we initially trained the entire neural network using a data set called ImageNet.[23] Afterward, we further refined the network's performance by adapting it to our specific OCTA image projections.

In detail, as shown in Figure 1, we used the EfficientNet[24] as the backbone with several necessary modifications. The first one is on the input end. Natural images usually have RGB (red–green–blue) three channels, while for our OCTA data, we consider SVC

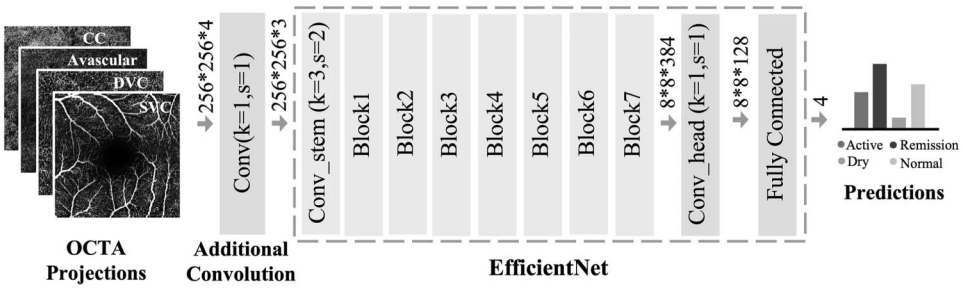

Fig. 1. Classifier structure for 2D en face OCTA projections. Layers in light gray scale have well pretrained weights while those in dark gray have to train from scratch.

(superficial vascular complex), deep vascular complex, avascular complex, and CC (choriocapillaris) four projections which take four channels. To handle this channel mismatch problem, we inserted an additional convolution layer with kernel size one in front of the EfficientNet to take 4-channel inputs and convert them to three channels. Second, considering that ImageNet has 1,000 categories while our task only needs four (active, remission, dry, and normal), we reduced the output channel of the last convolution layer from 1,536 to 128 to make the classifier more lightweight. Finally, we replaced the last fully connected layer with output size four to match the number of desired categories.

Note that in Figure 1, all three modified layers (shown in dark grey) are new ones without pretrained weights while the other layers (shown in light gray) are well-trained on natural images. If fine-tuned together, the new layers will disturb the tuning of the well pretrained layers. Therefore, we adopted a warmup step. We first froze all the layers with pretrained weights and trained the new layers only for 600 epochs. During this step, we also trained all the BatchNorm layers in the EfficientNet structure to better transfer from natural images distribution to OCTA projection distribution. Then, we fine-tuned all the layers together for another 900 epochs with a smaller learning rate.

For preparing the training data, we downsampled each OCTA projection from 512×512 to 256×256 as preprocessing. Then, we adopted several data augmentation methods to increase their diversity. In detail, we used random flipping, rotation, and cropping with resizing. We also randomly applied gamma transformation and Gaussian smooth to increase the diversity of intensity and used grid distortion to augment the shapes. During the network training, we adopted Adam optimizer with 0.00001 weight decay. The initial learning rate is 0.001 and decreased using a cosine scheduler with a minimum value of 0.00001. We used cosine loss as our optimization target, which is proved to be effective when handling small data amounts.[25]

We conducted a 5-fold validation experiment, where the training samples were partitioned into five equal-sized groups. For each fold, we picked one group of samples for validation and the other four groups for training. As a result, we obtained five different classifiers in each experiment. We regarded the ensemble classification results of these five classifiers as the final results to take the best usage of all the training samples. The ensemble strategy is averaging all five predictions from each fold.

Optical Coherence Tomography Angiography Human Expert Grading

512×512 OCTA images were graded by two masked retina specialists (C.M.B.G. and D.D.), who routinely use OCTA in clinical practice, based on the presence or absence of CNV on OCTA en face projections and masked to other images (SD-OCT B scan and OCT en face scan) and clinical information. These were different graders than two retina specialists labeling the data. Clinical decision-making was based on examination, and OCT B scan, not on OCTA scan. To clarify, the OCTA grading was performed by two other clinicians after the treatment was performed by the treating clinician. The treating clinician (W.R.F.) did not decide on treatment based on OCTA. The two masked graders had to predict the clinical category (A-active, R-remission, D-dry AMD, and N-normal) based on OCTA en face projections only (superficial vascular complex, deep vascular complex, avascular, and choriocapillaris). First, CNV was determined to be either present or absent based on standardized reference images consisting of en face structural OCTA of the superficial inner retinal plexus, deep inner retinal plexus, outer retina, and choriocapillaris for each eye. Images showing an apparent neovascular plexus in the avascular layer and/or in choriocapillaris were considered to indicate CNV. If vessels were identified, then graders were looking at their morphology and trying to grade the vessels as finely branching (presumably active) Figure 2 or less branching and more mature (predominantly inactive) Figure 3 based on characteristics previously described by Coscas et al[20] as a reference to help distinguish the clinical category.

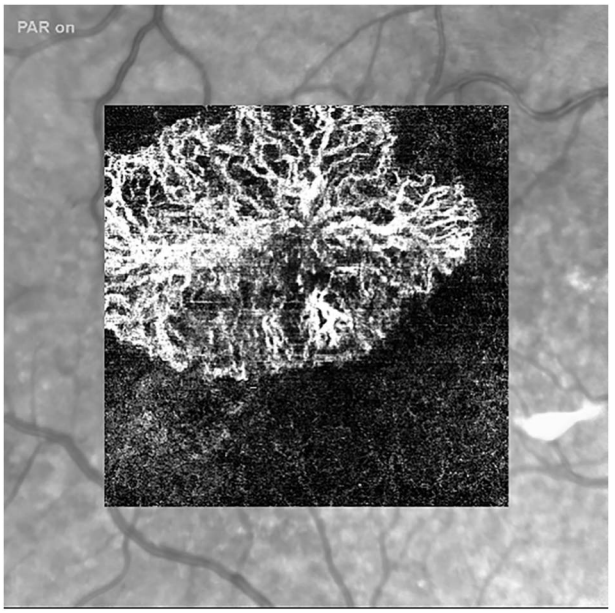

Fig. 2. OCTA en face projection of avascular layer in *active (exudative)*, untreated CNV with a highly visible network of tiny branching vessels and loops.

Figure 4, Aand B shows a reference image for OCTA in patient with dry AMD based on characteristics described by Arya et al.[26] Figure 5, Aand B represents a healthy subject with normal choriocapillaris and avascular layer in OCTA en face projection. Based on the above references and own clinical experience, a consensus grading between two experts were used for prediction of four categories. The two masked human graders used the same 56 test-set samples as the AI to predict the category.

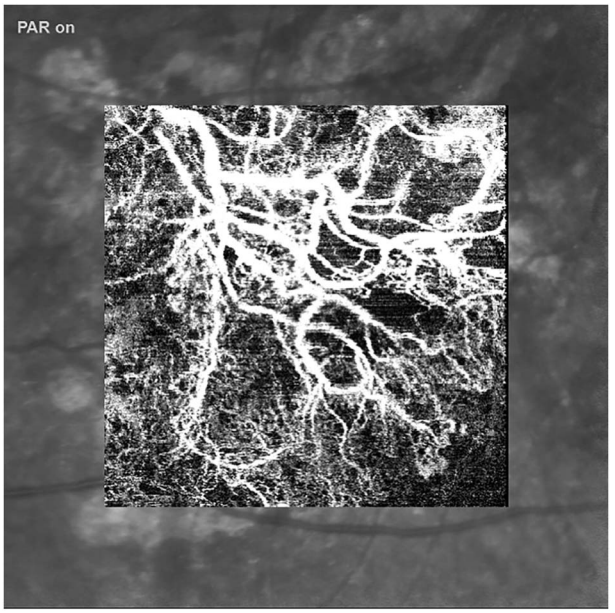

Fig. 3. OCTA en face projection of avascular layer shows *inactive* CNV (remission) with areas of dense vessels highly branched and longer matured vessels of large diameter anastomosing with sparse branching.

Statistical Analysis

Optical coherence tomography angiography en face images were classified either by AI or human retina experts into four categories in a masked fashion. Correct classification was coded as 1 and misclassified as 0. A logistic regression was performed with the classification method and disease categories as independent variables. Analysis was conducted by using SAS software version 14. Type I error was set as 5%, and comparisons were two-tailed.

Results

Artificial Intelligence Classifier Performance

We repeated the 5-fold validation experiment five times and obtained the classification accuracy 0.8036, 0.8036, 0.8393, 0.7679, and 0.7857 whose mean and SD are 0.80002 and 0.02648257918, respectively. Figure 6 shows the confusion matrix of the experiment with 0.8393 accuracy. According to this confusion matrix, we can calculate the sensitivity of these four categories as 0.7857 (active), 0.7142 (remission), 0.9286 (dry), and 0.9286 (normal), respectively. The corresponding specificities are 0.9524 for active, 0.9524 for remission, 0.9286 for dry, and 0.9524 for normal, respectively. We analyzed the performance of each category based on sensitivity and specificity.

Human Experts Grading Results

To fairly compare the human grading performance (2 masked experts) with AI prediction performance we have used the same testing data set (56 images) as the AI. Figure 7 shows the confusion matrix for predictive accuracy of clinical category by consensus of two human masked experts.

The sensitivity of prediction by human experts calculated based on this confusion matrix was: 0.4286 for active CNV, 0.2143 for remission CNV, 0.8571 for dry AMD, and 0.8571 for normal with specificity of 0.7619, 0.9286, 0.7857, and 0.9762 for these categories, respectively. Table 1 summarizes the results for sensitivity and specificity for category prediction for both AI and human. The comparison results of human and AI grading of OCTA scans is presented in Figure 8.

Overall, the AI classification prediction had significantly better accuracy than that by the human (Odds ratio = 1.95, P = 0.0021). Among four simplified

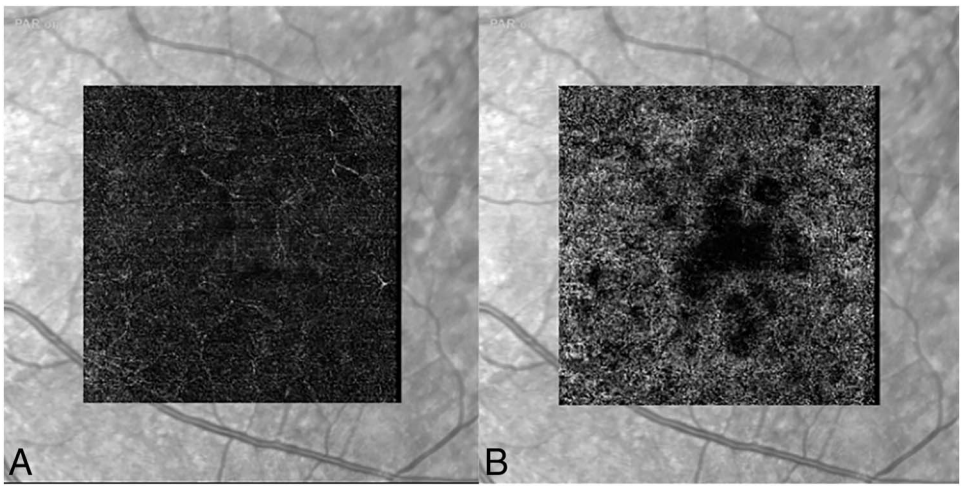

Fig. 4. (**A** and **B**) OCTA en face projection of dry AMD in avascular (**A**) and CC choriocapillaris layer (**B**). The avascular and CC layer show no neovascularization. In the CC layer, the areas of decreased flow (shadowing) correspond to areas beneath drusen and are well-visualized as dark oval-to-round areas.

categories of disease status, the probability of predictive accuracy was significantly different ($P = 0.0021$). Dry AMD and normal had a similar higher probability of prediction, the probability of which was 3.2 times higher than active lesion ($P = 0.0356$) or 6.5 times higher than lesions of remission ($P = 0.001$, Figure 8).

Discussion

In this study, we aimed to determine whether the AI can predict different stages of AMD disease and differentiate active from inactive, "nonleaking" CNV vessels in nAMD based on OCTA en face 2D projections only. Our DL-based algorithm was able to predict the disease stages with 80.36% average accuracy. The AI was significantly better in predicting the clinical classification in all categories (active CNV, wet AMD in remission, dry AMD, and normal) comparing with the human experts. Both AI and human graders did well in classifying normal and dry AMD based on OCTA only because there are no pathologic vessels visible in the avascular layer associated with this diagnosis. One of the OCTA characteristics that could help further distinguish the normal and dry AMD samples was the presence of flow voids in choriocapillaris associated with areas beneath drusen.[26] The highest sensitivity and specificity were achieved for dry and normal category (0.9286). This result matches our expectation. As discussed before, as a human, we know one sample belongs to dry or normal if there is no visible pathology in avascular and/or choriocapillaris projection. Then, the shadowing in CC projection (Fig. 4, Aand B) will further help us to decide the category. So, it is reasonable to achieve high performance on these two categories. By contrast, the lowest sensitivity was obtained for remission (0.7142) followed by active (0.7857). This means the active and remission categories are difficult to distinguish based on only OCTA en face projections judging from vessel pattern and morphology,

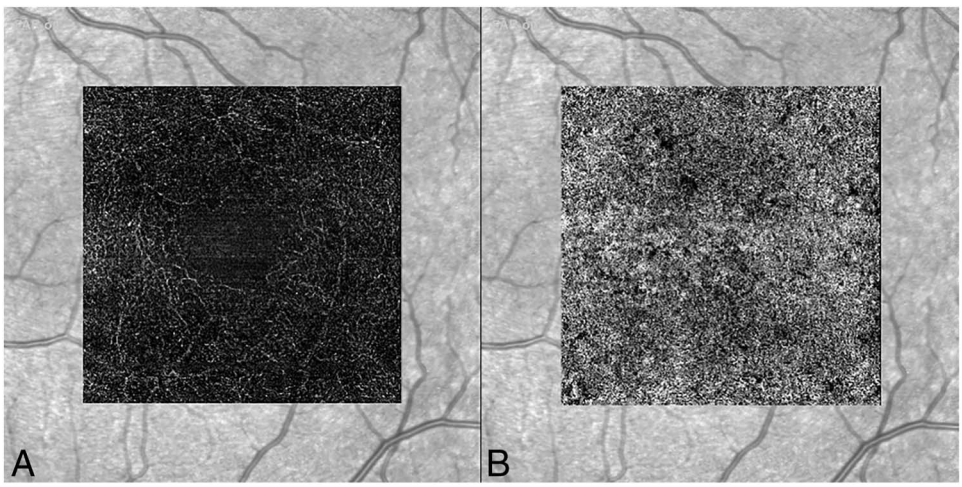

Fig. 5. (**A** and **B**) OCTA en face projection of avascular layer (**A**) and choriocapillaris (**B**) of healthy subject without AMD or neovascular activity.

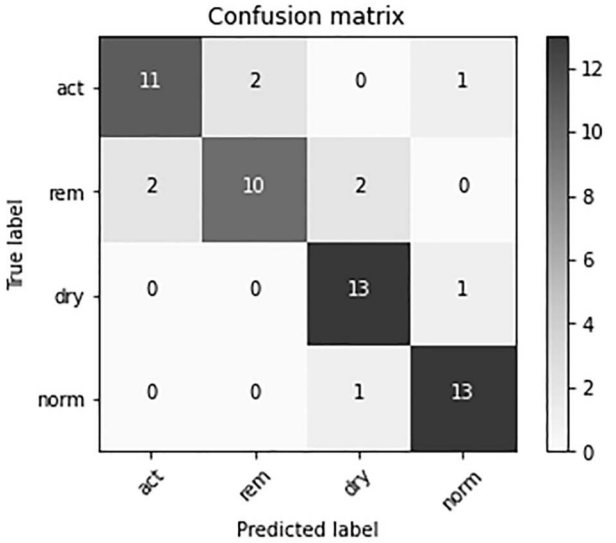

Fig. 6. Confusion matrix of the experiment shows 0.8393 accuracy of overall AI prediction.

and this result is consistent with the observation of human graders.

The most challenging task for both AI and human graders was to distinguish the category of the CNV vessels (active meaning "leaking" vessels vs. inactive meaning "nonleaking," vessels, sometimes called CNV in remission or being suppressed by chronic treatment). The AI did significantly better in predicting the vessel category compared with human experts. It is unknown how the AI can distinguish the active from inactive CNV vessels. Deep learning may help in clinician-driven automated discovery of novel disease biomarkers.

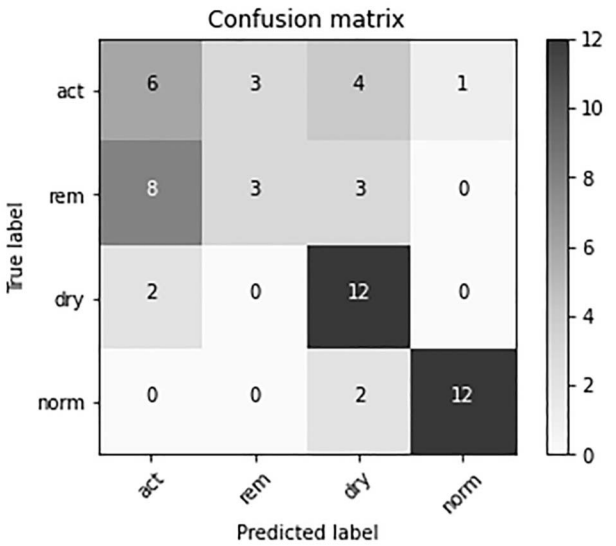

Fig. 7. Confusion matrix for the human expert's prediction accuracy of four clinical categories.

In our study, the task was not only to distinguish normal subjects from AMD disease, but within the eyes with nAMD, the algorithm showed high sensitivity in predicting the active CNV (0.7857). The sensitivity for remission (inactive CNV vessels) was the lowest of all four categories (0.7142). There are several possible reasons for that. The first could be the presence of some segmentation errors. Although, in our study, we have eliminated the samples with poor quality and gross and minor segmentation errors were corrected manually, if needed, on the Bruch membrane (BM) layer, the presence of projection artifacts and other segmentation errors could affect the AI predictive performance and cause misclassification because some fine-vessel branching could be missed or not visualized. Other authors have shown that manual modification of the position of automatically generated segmentation lines anterior and posterior to any suspected CNV (subretinal hyper-reflective material or pigment epithelial detachment) increases the sensitivity of CNV detection compared with automatically generated slabs.[27] Other publications have also recognized the importance of segmenting BM. Failure to accurately segment BM can substantially alter both qualitative and quantitative analysis of choriocapillaris.[28] Based on these findings, our group segmented the BM only. Nevertheless, the fact of not correcting other retinal layers could be a limitation of this study and the influence of that on CNV visualization should be further investigated in future studies. Certainly, the novel AI-based segmentation algorithms will be helpful in this matter and could be applied in the future to improve classification performance.[29]

The lower success rate of prediction performance in the active and remission CNV category could be also associated with limitations of OCTA as an imaging modality, or the fact that in some patients, the morphology of the CNV vasculature does not change despite lack of leakage. Slow flow or pooling in vessels may potentially cause that the motion is not captured and the vessels are missed. As reported in previous studies, the sensitivity and specificity for CNV detection using OCTA vary from 50% to 86.5% sensitivity to 67.6% to 100% specificity, respectively.[8,9,20,30]

Coscas and other authors[19,20] have shown that quantitative OCTA biomarkers (vessel length, branching index, and vessel density) may have predictive value for lesion activity. However, those studies show an imperfect correlation as well. Our algorithm results in a relatively high sensitivity and specificity to predict the clinical status of patients with AMD based on OCTA vascular en face projections alone. This suggests that vascular morphology can help predict disease state and should be studied at different stages of

Table 1. Results for Sensitivity and Specificity for AMD Category Prediction for Both AI and Human

Category	Sensitivity (AI)	Specificity (AI)	Sensitivity (Human)	Specificity (Human)
Active CNV	0.7857	0.9524	0.4286	0.7619
CNV in remission	0.7142	0.9524	0.2143	0.9286
Dry AMD	0.9286	0.9286	0.8571	0.7857
Normal	0.9286	0.9524	0.8571	0.9762

neovascular AMD and under treatment with different drug regimens. It is important to note that there are false positives and negatives that may result from poor visualization of vessels because of thick or opaque fluid or blood. In addition, layer segmentation errors and artifacts may lead to both false-negative and false-positive results. False-positive results may be due to the geographic atrophy and hypertransmission of the signal showing choroid vessels in the avascular area. These can be usually eliminated by correcting the segmentation error of BM. Hence, there are situations where we clinically expect to see the CNV vessels in OCTA based on FA leakage and fluid in SD-OCT, but we do not find them, even after the elimination of segmentation errors and artifacts. Other cases exist where we observe no fluid in SD-OCT and a lack of leakage in FA, but we appreciate the persisting CNV vessels detected in OCTA. These vessels in our study were classified under the remission category of nAMD and they include patients treated with anti-VEGF who do not show fluid in SD-OCT. Several groups attempted to explain the presence of CNV vessels in OCTA in eyes treated with anti-VEGF. Gong et al[30] suggest that the structure of the central subretinal neovascular trunk may differ from that of the surrounding finer plexus and may be more resistant to anti-VEGF therapy because the endothelial cells are protected by overlying pericytes. They also suggest that smaller branching vessels consist of unprotected endothelial cells, which are more responsive to anti-VEGF therapy. Coscas et al[20] had previously described the activity criteria of CNV using OCTA. The direct visualization of key pathophysiologic features of neovascular AMD, that is the CNV component, may allow us to better understand the pathology and strongly affect the treatment decisions.

The use of AI in longitudinal studies on big OCTA data could help in understanding the changes in CNV morphology during therapy in nAMD using different drugs and various treatment regimens to predict the

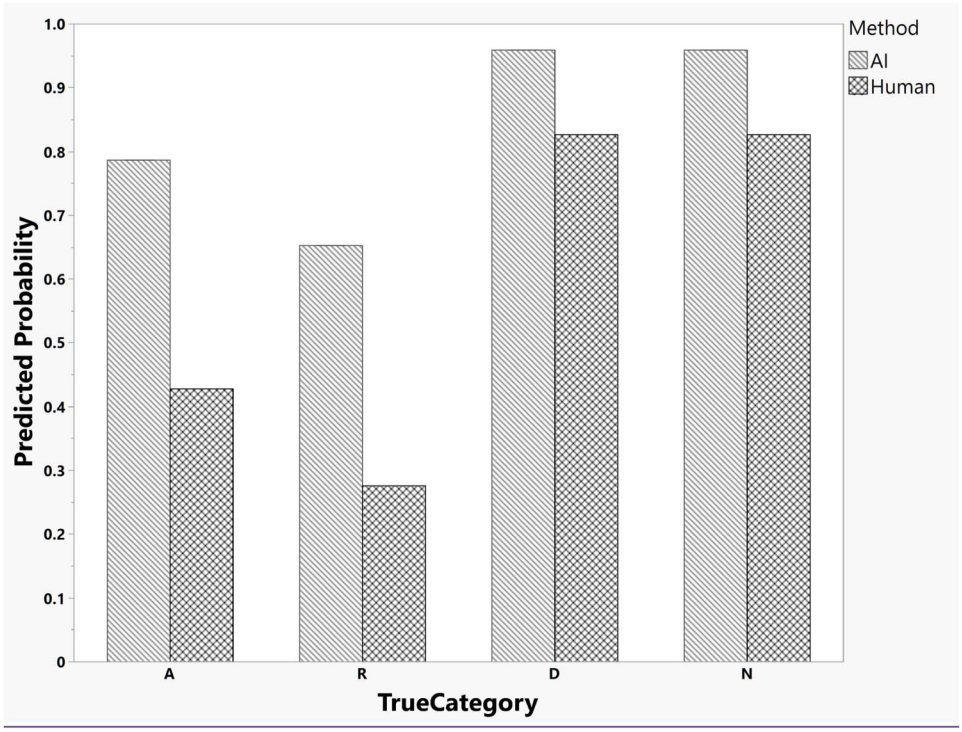

Fig. 8. The bar graph shows the predicted probability for each category (A-active AMD, R-remission, D-dry AMD, and N-normal, without AMD) stratified by AI and human grading. Overall, the AI classification prediction is significantly better than the human.

therapeutic success and design patients' personalized treatment. The quantitative and qualitative changes of vessels in CNV visualized with OCTA could be an end point of clinical trials designing new drugs targeting those persisting CNV vessels, and using the AI would be a helpful tool in automated analysis of these parameters. It is known, that even when the fluid regressed, the underlying pathologic vessels may still be present, and OCTA is currently the only imaging tool that is able to visualize them. Our DL model shows a high prediction accuracy for clinical diagnosis based on OCTA en face projections only and did better than experienced ophthalmologists. This is to the best of our knowledge, the first report of AI-based clinical classification in AMD using the OCTA en face projections only. Using our DL model could help in predicting the diagnosis and support decision-making in areas where there is lack of qualified retina specialists. Adding additional information to the platform, such as SD-OCT, would certainly increase the prediction accuracy, having all the necessary information about the disease activity. We have shown that DL has high potential in disease classification based on OCTA vessel morphology only and could be used in supporting the diagnosis and treatment of nAMD. With longitudinal observation and additional clinical information such as vision and treatment regimen, it could help predicating the therapeutical outcome of anti-VEGF therapy in nAMD.

Conclusion

Our AI algorithm is a successful prediction tool of disease classification in AMD based on OCTA 2-D en face vascular projections only, even without information about fluid in SD-OCT. In our study, the AI prediction accuracy was significantly higher than that of consensus of two human experts. Our model can be used in the automated process of disease diagnosing and supporting decision-making in nAMD and a helpful tool for monitoring clinical trials end points in designing new treatment strategies of wet AMD targeting persisting CNV vessels.

It is well-known that the gold standard in imaging and decision-making in nAMD is the OCT B scan with clinical information about the fluid and FA showing leakage. We have demonstrated that the vessel morphology-based solely on OCTA can predict the disease activity. In the future, our data suggest that the AI will be able to combine all the clinical information about the vessel morphology, fluid in SD-OCT, and drug used for treatment to predict the treatment intervals, outcome vision, and therapeutic success using the specific drug. Because AI can predict vascular activity better than human observation alone, it will be a useful tool in building analytic models of CNV and AMD disease activity and in permitting a better understanding of treatment and treatment efficacy in neovascular AMD.

Key words: age-related macular degeneration, artificial intelligence, classification prediction, CNV, deep learning, image analysis, OCTA.

Acknowledgments

The authors acknowledge Varsha Alex M.D. for contributing to data collection.

References

1. Spaide RF, Fujimoto JG, Waheed NK, et al. Optical coherence tomography angiography. Prog Retin Eye Res 2018;64:1–55.
2. Friedman E. Choroidal neovascularization and age-related macular degeneration. Ophthalmology 1999;106:647.
3. Lim LS, Mitchell P, Seddon JM, et al. Age-related macular degeneration. Lancet 2012;379:1728–1738.
4. Heinke A, Freeman WR, Bartsch D-UG, et al. Quantitative evaluation of morphological changes in anti-VEGF treated choroidal neovascularization due to age related macular degeneration using optical coherence tomography angiography. Invest Ophthalmol Vis Sci 2022;63:1348.
5. Hormel TT, Huang D, Jia Y. Artifacts and artifact removal in optical coherence tomographic angiography. Quant Imaging Med Surg 2021;11:1120–1133.
6. Zhang H, Heinke A, Galang C, et al. Robust AMD Stage Grading with Exclusively OCTA Modality Leveraging 3D Volume. Proceedings of the IEEE/CVF International Conference on Computer Vision2023.
7. Schneider EW, Fowler SC. Optical coherence tomography angiography in the management of age-related macular degeneration. Curr Opin Ophthalmol 2018;29:217–225.
8. de Carlo TE, Bonini Filho MA, Chin AT, et al. Spectral-domain optical coherence tomography angiography of choroidal neovascularization. Ophthalmology 2015;122:1228–1238.
9. Faridi A, Jia Y, Gao SS, et al. Sensitivity and specificity of OCT angiography to detect choroidal neovascularization. Ophthalmol Retina 2017;1:294–303.
10. Cavichini M, Dans KC, Jhingan M, et al. Evaluation of the clinical utility of optical coherence tomography angiography in age-related macular degeneration. Br J Ophthalmol 2021;105:983–988.
11. Heiferman MJ, Fawzi AA. Progression of subclinical choroidal neovascularization in age-related macular degeneration. PLoS One 2019;14:e0217805.
12. Hormel TT, Hwang TS, Bailey ST, et al. Artificial intelligence in OCT angiography. Prog Retin Eye Res 2021;85:100965.
13. Burlina PM, Joshi N, Pekala M, et al. Automated grading of age-related macular degeneration from color fundus images using deep convolutional neural networks. JAMA Ophthalmol 2017;135:1170–1176.
14. Camino A, Jia Y, Yu J, et al. Automated detection of shadow artifacts in optical coherence tomography angiography. Biomed Opt Express 2019;10:1514–1531.

15. Alqudah AM. AOCT-NET: a convolutional network automated classification of multiclass retinal diseases using spectral-domain optical coherence tomography images. Med Biol Eng Comput 2020;58:41–53.
16. Vaghefi E, Hill S, Kersten HM, Squirrell D. Multimodal retinal image analysis via deep learning for the diagnosis of intermediate dry age-related macular degeneration: a feasibility study. J Ophthalmol 2020;2020:7493419.
17. Jin K, Yan Y, Chen M, et al. Multimodal deep learning with feature level fusion for identification of choroidal neovascularization activity in age-related macular degeneration. Acta Ophthalmol 2022;100:e512–e520.
18. Thakoor KA, Yao J, Bordbar D, et al. A multimodal deep learning system to distinguish late stages of AMD and to compare expert vs. AI ocular biomarkers. Sci Rep 2022;12:2585.
19. Kalra G, Zarranz-Ventura J, Chahal R, et al. Optical coherence tomography (OCT) angiolytics: a review of OCT angiography quantitative biomarkers. Surv Ophthalmol 2022;67:1118–1134.
20. Coscas GJ, Lupidi M, Coscas F, et al. Optical coherence tomography angiography versus traditional multimodal imaging in assessing the activity of exudative age-related macular degeneration: a new diagnostic challenge. Retina 2015;35:2219–2228.
21. Gershoni A, Barayev E, Vainer I, et al. Thickness measurements taken with the spectralis OCT increase with decreasing signal strength. BMC Ophthalmol 2022;22:148.
22. Montolío A, Cegoñino J, Garcia-Martin E, Pérez Del Palomar A. Comparison of machine learning methods using spectralis OCT for diagnosis and disability progression prognosis in multiple sclerosis. Ann Biomed Eng 2022;50:507–528.
23. Deng J, Dong W, Socher R, et al. ImageNet: A Large-Scale Hierarchical Image Database. IEEE Conference on Computer Vision and Pattern Recognition 2009:248–255.
24. Tan MaL. Q.V. EfficientNet: Rethinking Model Scaling for Convolutional Neural Networks. Int conference on machine learning 6105–14.
25. Barz B, Denzler J. Deep Learning on Small Datasets Without Pre-training Using Cosine Loss. Proceedings of the IEEE/CVF Winter Conference on Applications of Computer Vision; 2020.
26. Arya M, Sabrosa AS, Duker JS, Waheed NK. Choriocapillaris changes in dry age-related macular degeneration and geographic atrophy: a review. Eye Vis (Lond) 2018;5:22.
27. Siggel R, Spital C, Lentzsch A, Liakopoulos S. Comparison of automated versus manually modified OCT angiography en face slabs for detection of choroidal neovascularization. Ophthalmol Retina 2020;4:471–480.
28. Schottenhamml J, Moult EM, Ploner SB, et al. OCT-OCTA segmentation: combining structural and blood flow information to segment Bruch's membrane. Biomed Opt Express 2021;12:84–99.
29. Wang Y, Galang C, Freeman WR, et al. Retinal OCT layer segmentation via joint motion correction and graph-assisted 3D neural network. IEEE Access 2023;11:103319–103332.
30. Gong J, Yu S, Gong Y, et al. The diagnostic accuracy of optical coherence tomography angiography for neovascular age-related macular degeneration: a comparison with fundus fluorescein angiography. J Ophthalmol 2016;2016:7521478.